


Obtaining efficient collisional engines via velocity-dependent drivings

Iago N. Mamede , Angel L. L. Stable, and C. E. Fiore *Universidade de São Paulo, Instituto de Física, Rua do Matão, 1371, 05508-090 São Paulo, SP, Brazil*

(Received 9 September 2022; accepted 30 November 2022; published 19 December 2022)

Brownian particles interacting sequentially with distinct temperatures and driving forces at each stroke have been tackled as a reliable alternative for the construction of engine setups. However, they can behave very inefficiently depending on the driving used for the work source and/or when temperatures of each stage are very different from each other. Inspired by some models for molecular motors and recent experimental studies, a coupling between driving and velocities is introduced and detail investigated from stochastic thermodynamics. Exact expressions for thermodynamic quantities and distinct maximization routes have been obtained. The search of an optimal coupling provides a substantial increase of engine performance (mainly efficiency), even for large ΔT . A simple and general argument for the optimal coupling can be estimated, irrespective of the driving and other model details.

DOI: [10.1103/PhysRevE.106.064125](https://doi.org/10.1103/PhysRevE.106.064125)

I. INTRODUCTION

One of the main goals of nonequilibrium thermodynamics is to understand, from an operational point of view, the conversion between distinct amounts of energy into useful power output [1]. Such a fundamental issue appears in several systems in nature, encompassing physical [2–5], biological [6,7], chemical processes [8], quantum technologies, and others, and thereby illustrating the great deal of attention devoted to describing thermal machines operating at the nanoscale [2,3]. Among the distinct setups, we cite those composed of quantum dots [9], colloidal particles [4,5,10], single [11] and coupled systems [12,13] acting as working substance and others [14]. Most of the above examples deal with engines operating under fixed or time-periodic variation of external parameters.

Collisional machines have also been tackled as a candidate for the construction of reliable thermal engines, in which the system is sequentially exposed to a distinct thermal reservoir and external driving forces and the time required for switching the thermal baths at the end of each stage is neglected. More recently, such idea of engines has been proposed and extended for Brownian engines, in which at each stage a particle is subjected to a distinct driving work source. Despite its reliability in distinct situations, such as systems interacting only with a small fraction of the environment or those presenting distinct drivings over each member of the system [15–18], such class of systems can operate inefficiently depending on the way it is projected (temperatures, kind of driving, and duration of each stroke). For this reason, recent strategies, such as optimal switching time between thermal baths [19,20] and the choice of an appropriate driving [21] at each stroke have been proposed and investigated. However, about improvements can be limited when heat cannot be converted into output work and the temperature difference ΔT between strokes increases, yielding small efficiencies [20–22].

Aimed at circumventing the above limitation, we introduce a new ingredient as an strategy for improving the efficiency of

Brownian thermal engines. It consists of including a velocity dependent driving in which the output power generation is due to two component drivings: the first, given by $f_i h_i(t)$, is coming from an arbitrary driving $h_i(t)$ with strength f_i , whereas the second, given by $\alpha f_i v_i$, accounts to the coupling between the driving strength and velocity v_i , where parameter α quantifies its weight. Driving forces proportional to the velocity are rarely explored theoretically [23,24], but they are present in distinct experimental studies such as an electrical force stemming from delayed feedback [25], self-motile colloidal particles [26], catalytic nanomotors [27], and others [28]. Our results reveal that the search of an optimal coupling provides a substantial increase of engine performance (mainly efficiency), even for a large difference of temperatures.

This paper is organized as follows. Section II presents the main equations, system thermodynamics, and distinct optimization routes. Results and phase diagrams are presented in Sec. III and conclusions are drawn in Sec. IV.

II. THERMODYNAMICS OF COLLISIONAL ENGINES

One of the simplest nanoscopic engines is composed of a Brownian particle with mass m sequentially placed in contact with a given thermal reservoir and subjected to an external force $\tilde{f}_i(t)$ at each stage. Each contact has a duration of τ/N (with τ and N being the total time and the number of strokes, respectively) and occurs during the intervals $\tau_{i-1} \leq t < \tau_i$, where $\tau_i = i\tau/N$ for $i = 1, \dots, N$, in which the particle evolves in time according to the following Langevin equation:

$$\frac{dv_i}{dt} = -\gamma_i v_i + \tilde{f}_i(t) + \xi_i(t), \quad (1)$$

where quantities v_i , γ_i , and $\tilde{f}_i(t)$ denote its velocity, the viscous constant, and the driving force, respectively. As stated previously, we propose $\tilde{f}_i(t)$ as given by the time dependent plus a velocity dependent components $\tilde{f}_i(t) = [h_i(t) - \alpha v_i] f_i$, where α is a constant. Note that one recovers the

standard collisional engine as $\alpha = 0$ [20,22]. The interaction between particle and the i th environment is described by the white-noise stochastic force $\xi_i(t)$, satisfying the white-noise properties:

$$\langle \xi_i(t) \rangle = 0, \quad \langle \xi_i(t) \xi_i(t') \rangle = 2\gamma_i T_i \delta_{ii'} \delta(t - t'), \quad (2)$$

where T_i is the bath temperature. In order to derive the thermodynamics, let $P_i(v, t)$ be the velocity probability distribution with time evolution described by the Fokker-Planck (FP) equation [29–32]:

$$\frac{\partial P_i}{\partial t} = -f_i h_i(t) \frac{\partial P_i}{\partial v} - \frac{\partial J_i}{\partial v_i}, \quad (3)$$

where J_i is given by

$$J_i = -\beta_i v_i P_i - \gamma_i T_i \frac{\partial P_i}{\partial v_i}, \quad (4)$$

where $\beta_i = \gamma_i + \alpha f_i$. Note that the term αf_i is the new quantity to be optimized, together with the external force f_i . For simplifying matters, from now on, we shall assume $k_B = m = 1$.

From the FP equation and by performing the usual boundary conditions in the space of velocities, in which both $P_i(v, t)$ and $J_i(v, t)$ vanish as $|v| \rightarrow \infty$, the first and second law of thermodynamics can be derived. Starting with the former, the time variation of the energy system $U_i = \langle E_i \rangle$ is given by $dU_i/dt = -(\dot{W}_i + \dot{Q}_i)$, where $\dot{W}_i(t)$ and $\dot{Q}_i(t)$ denote the work per unity of time (power) and heat flux exchanged between the system and the environment (thermal bath) reading

$$\dot{W}_i(t) = -f_i \langle v_i \rangle(t), \quad \dot{Q}_i(t) = \beta_i \langle v_i^2 \rangle(t) - \gamma_i T_i, \quad (5)$$

respectively. Analogously, time evolution of system entropy $S_i(t) = -\ln[P_i(v_i, t)]$ is given by

$$\frac{dS_i}{dt} = \frac{1}{\gamma_i T_i} \left[\int \frac{J_i^2}{P_i} dv_i + \beta_i \int v_i J_i dv_i \right], \quad (6)$$

where the first and second right terms are identified as the entropy production rate $\Pi_i(t)$ and entropy flux $-\Phi_i(t)$, respectively [30–32]. Note that $\Pi_i(t) \geq 0$ (as expected), whereas $\Phi_i(t)$ can be rewritten in a more convenient way:

$$\Phi_i(t) = \frac{\beta_i}{\gamma_i T_i} [\beta_i \langle v_i^2 \rangle(t) - \gamma_i T_i]. \quad (7)$$

Summarizing, the above expressions for thermodynamic quantities can be calculated from ensemble averages $\langle v_i \rangle(t)$ and $\langle v_i^2 \rangle(t) = b_i(t) + \langle v_i \rangle(t)^2$. Since the coupling between velocity and external driving has been incorporated into Eq. (4), the probability distribution has a similar form to the couplingless case [22] and is a Gaussian:

$$P_i(v, t) = \frac{1}{\sqrt{2\pi b_i(t)}} \exp\left(-\frac{1}{2b_i(t)} [v - \langle v_i \rangle(t)]^2\right), \quad (8)$$

in which the mean $\langle v_i \rangle(t)$ and variance $b_i(t) = \langle v_i^2 \rangle(t) - \langle v_i \rangle(t)^2$ are time dependent and obey the following equations:

$$\frac{d\langle v_i \rangle(t)}{dt} = -\beta_i \langle v_i \rangle(t) + f_i h_i(t) \quad (9)$$

and

$$\frac{db_i(t)}{dt} = -2\beta_i b_i(t) + 2\gamma_i T_i, \quad (10)$$

respectively. Continuity of $P_i(v, t)$ at each stroke implies that $P_i(v, \tau_i) = P_{i+1}(v, \tau_i)$ (for all $i = 1, \dots, N$). Since the system must return to the initial state after a complete cycle, it follows that $P_N(v, \tau) = P_1(v, 0)$. The above conditions are only satisfied if $\langle v_i \rangle(\tau_i) = \langle v_{i+1} \rangle(\tau_i)$ and $b_i(\tau_i) = b_{i+1}(\tau_i)$ (for all $i = 1, \dots, N$); together $\langle v_1 \rangle(0) = \langle v_N \rangle(\tau)$ and $b_1(0) = b_N(\tau)$ and therefore all averages $\langle v_i \rangle(t)$'s and variances can be solely calculated in terms of model parameters, that is, from the driving, temperature reservoirs, coupling α , and the period. By focusing on the simplest design of an engine composed of only two strokes, expressions for averages and variances can be obtained for an arbitrary driving:

$$\langle v_1 \rangle(t) = e^{-\beta_1 t} \left(f_1 \mathcal{F}_1(t, \alpha) + \frac{f_2 e^{\frac{\beta_1 \tau}{2}} \mathcal{F}_2(\tau, \alpha) + f_1 \mathcal{F}_1(\frac{\tau}{2}, \alpha)}{e^{\frac{\tau}{2}(\beta_1 + \beta_2)} - 1} \right) \quad (11)$$

and

$$\langle v_2 \rangle(t) = e^{-\beta_2(t - \frac{\tau}{2})} \times \left(f_2 \mathcal{F}_2(t, \alpha) + \frac{f_1 e^{\frac{\beta_2 \tau}{2}} \mathcal{F}_1(\frac{\tau}{2}, \alpha) + f_2 \mathcal{F}_2(\tau, \alpha)}{e^{\frac{\tau}{2}(\beta_1 + \beta_2)} - 1} \right) \quad (12)$$

for the mean velocities and

$$b_1(t) = \frac{\gamma(e^{\beta_2 \tau} - 1)(\beta_1 T_2 - \beta_2 T_1)e^{-2\beta_1(t - \tau/2)} + \gamma T_1}{\beta_1 \beta_2 (e^{(\beta_1 + \beta_2)\tau} - 1)} + \frac{\gamma T_1}{\beta_1} \quad (13)$$

and

$$b_2(t) = \frac{\gamma(e^{\beta_1 \tau} - 1)(\beta_2 T_1 - \beta_1 T_2)e^{\beta_2 \tau - 2\beta_2(t - \frac{\tau}{2})} + \gamma T_2}{\beta_1 \beta_2 (e^{(\beta_1 + \beta_2)\tau} - 1)} + \frac{\gamma T_2}{\beta_2} \quad (14)$$

for variances, respectively, where $\mathcal{F}_1(t, \alpha) = \int_0^t e^{\beta_1 t'} h_1(t') dt'$ and $\mathcal{F}_2(t, \alpha) = \int_{\tau/2}^t e^{\beta_2(t' - \frac{\tau}{2})} h_2(t' - \frac{\tau}{2}) dt'$ are arbitrary functions representing the contribution of time dependent drivings. The above expressions allow the calculation of all thermodynamic quantities. Starting with the work (actually the power) definition given by the left side of Eq. (5) together with Eqs. (11) and (12) averaged over a complete period, its expression in the first and second stages are given, respectively, by

$$\overline{\dot{W}}_1 = -\frac{f_1}{\tau} \int_0^{\frac{\tau}{2}} h_1(t) e^{-(\gamma + \alpha f_1)t} \times \left(f_1 \mathcal{F}_1(t, \alpha) + \frac{f_2 e^{\frac{(\gamma + \alpha f_1)\tau}{2}} \mathcal{F}_2(\tau, \alpha) + f_1 \mathcal{F}_1(\frac{\tau}{2}, \alpha)}{e^{\frac{\tau}{2}[2\gamma + (f_1 + f_2)\alpha]} - 1} \right) dt \quad (15)$$

and

$$\overline{\dot{W}}_2 = -\frac{f_2}{\tau} \int_{\frac{\tau}{2}}^{\tau} h_2(t) e^{-(\gamma + \alpha f_2)(t - \frac{\tau}{2})} \times \left(f_2 \mathcal{F}_2(t, \alpha) + \frac{f_1 e^{\frac{(\gamma + \alpha f_2)\tau}{2}} \mathcal{F}_1(\frac{\tau}{2}, \alpha) + f_2 \mathcal{F}_2(\tau, \alpha)}{e^{\frac{\tau}{2}[2\gamma + (f_1 + f_2)\alpha]} - 1} \right) dt \quad (16)$$

and, respectively, hold valid for all periods and time dependent drivings $f_i h_i(t)$'s. In contrast to collisional engines in which $\alpha = 0$ [20,22], they do not present a quadratic dependence on forces f_1 and f_2 , but reduce to them in such a limit.

Analogously, having expressions for $\langle v_1^2 \rangle(t)$ and $\langle v_2^2 \rangle(t)$, averages \bar{Q}_1 (\bar{Q}_2) are obtained as a sum of two terms: $\bar{Q}_1 = \bar{Q}_{1f} + \bar{Q}_{f_1, f_2, T_1}$ ($\bar{Q}_2 = \bar{Q}_{2f} + \bar{Q}_{f_1, f_2, T_2}$); the former component

$$\bar{Q}_{f_1, f_2, T_1} = \frac{(e^{(1+\alpha f_1)\tau} - 1)(e^{(1+\alpha f_2)\tau} - 1)[\alpha(f_1 T_2 - f_2 T_1) + T_2 - T_1]}{2\tau(e^{\tau[\alpha(f_1+f_2)+2]} - 1)(1 + \alpha f_1)(1 + \alpha f_2)} \quad (17)$$

and $\bar{Q}_{f_1, f_2, T_1} = -\bar{Q}_{f_1, f_2, T_2}$. Due to the continuity of the probability distribution, it follows that $U_1(\tau/2) = U_2(\tau/2)$ and $U_2(\tau) = U_1(0)$ and therefore $\bar{Q}_1 + \bar{Q}_2 + \bar{W}_1 + \bar{W}_2 = 0$, in consistency with the first law of thermodynamics. Finally, having \bar{Q}_i 's, the steady entropy production is promptly obtained from Eq. (7) and given by $\bar{Q}_1/T_1 + \bar{Q}_2/T_2$.

A. Constant and linear drivings

In order to compare our new ingredient with previous collisional engines [20–22], analysis will be exemplified for the two simplest kinds of drivings: constant and linear ones. Both of them have strengths f_1 and f_2 , with the former being time independent at $0 < t \leq \tau/2$ and $\tau/2 < t \leq \tau$, respectively, whereas the latter is given by

$$h_i(t) = \begin{cases} \gamma t, & 0 \leq t < \tau/2, \\ \gamma(t - \tau/2), & \tau/2 \leq t < \tau. \end{cases} \quad (18)$$

Thermodynamic quantities are directly evaluated from Eqs. (16) and (17). Previous works have shown that both drivings can be used for projecting the system as an engine, in which the constant driving is always more advantageous for enhancing the power output and efficiency and such latter one substantially decreasing upon the difference of temperature increases.

B. Efficiency

In several cases, the entropy production assumes the generic bilinear form $J_1 F_1 + J_d F_d$. It has been used for describing several models in nonequilibrium thermodynamics, such as linear stochastic thermodynamics [2,11,33], systems in contact presenting a single work source and heat source [34], work-to-work transducers [6,7,35–37], and others. A common definition of efficiency in such cases is given by the ratio between entropy production components $-J_1 F_1 / J_d F_d$, describing the partial conversion of one type of energy, expressed in terms of a driving force F_d with corresponding flux J_d into another one, characterized by a load force F_1 and flux J_1 . On the other hand, the class of engines we are investigating can be associated with three thermodynamic forces (two of them are related to f_1 , f_2 and the third with the difference of temperatures), implying the usage of the above ratio as a dubious measure of the system performance for $T_1 \neq T_2$. For this reason, we consider a definition of efficiency given by

is given by $\bar{Q}_{1f} = \int_0^{\tau/2} \langle v_1 \rangle^2(t) dt / \tau$ [$\bar{Q}_{2f} = \int_{\tau/2}^{\tau} \langle v_2 \rangle^2(t) dt / \tau$] and accounting to the contribution for heat due to drivings, whereas the latter \bar{Q}_{f_1, f_2, T_1} reads $\bar{Q}_{f_1, f_2, T_1} = \int_0^{\tau/2} b_1(t) dt / \tau - \frac{\gamma T_1}{2}$ and describes the interplay between strength forces f_i 's, temperatures of reservoirs T_i 's, and α . From expressions for $b_i(t)$'s, each above component is given by

[13,20,21]

$$\eta = -\frac{\mathcal{P}}{\bar{W}_1 + \bar{Q}_1 \Theta(-\bar{Q}_1) + \bar{Q}_2 \Theta(-\bar{Q}_2)}, \quad (19)$$

also expressing the partial conversion of a given amount of energy under the form of input heat $\bar{Q}_1 \Theta(-\bar{Q}_1) + \bar{Q}_2 \Theta(-\bar{Q}_2) < 0$ [$\Theta(x)$ being the Heaviside function] plus input work $\bar{W}_1 < 0$ into power output $\mathcal{P} \equiv \bar{W}_2 \geq 0$. Equation (19) reduces to the previous definition for $\Delta T = T_1 - T_2 = 0$ in which output and input works are related to fluxes as $\mathcal{P} = -T J_1 F_1$ and $\bar{W}_1 = -T J_d F_d$ [11,13,21,22]. Since realistic engines operate at finite time, we are going to exploit distinct routes for optimizing the system performance for finite τ : by maximizing η and \mathcal{P} with respect to the f_2/f_1 and α . Although they can be directly performed from the expressions for \mathcal{P} and η from Eqs. (16) and (19), respectively, expressions for maximized quantities may be little instructive, due to the complex interplay between α and f_2 . For this reason, in the next section, we shall present distinct approaches and reasonings for obtaining some maximized quantities with respect to α (for fixed ratio f_2/f_1 , here undertaken by taking f_2 fixed and $f_1 = 1$) and optimized f_2 (for fixed α and f_1).

C. Linear approximation for the power output

In order to obtain some insight into the interplay between α , f_i 's, and T_i 's, a linear analysis will be performed for small α , in which the average \mathcal{P} is decomposed in the following way:

$$\mathcal{P} \approx \mathcal{P}_0 + \alpha \mathcal{P}_\alpha, \quad (20)$$

where \mathcal{P}_0 accounts for the average power (calculated at the second stage) for the couplingless case. According to Refs. [20,21], \mathcal{P}_0 can be expressed in terms of Onsager coefficients, $\mathcal{P}_0 = -T_2(L_{21}f_1 + L_{22}f_2)f_2$, where each coefficient L_{2i} is given by

$$L_{22} = \frac{m}{T_2 \tau (e^{\gamma \tau} - 1)} \left[\int_{\tau/2}^{\tau} h_2(t) e^{-\gamma t} dt \int_{\tau/2}^{\tau} h_2(t') e^{\gamma t'} dt' + (e^{\gamma \tau} - 1) \int_{\tau/2}^{\tau} h_2(t) e^{-\gamma t} \int_{\tau/2}^t h_2(t') e^{\gamma t'} dt' dt \right],$$

$$L_{21} = \frac{m e^{\gamma \tau}}{T_2 \tau (e^{\gamma \tau} - 1)} \int_0^{\tau/2} h_1(t') e^{\gamma t'} dt' \int_{\tau/2}^{\tau} h_2(t) e^{-\gamma t} dt. \quad (21)$$

In a similar fashion, expressions for the average work in the first stage assume the form $\overline{W}_{10} = -T_1(L_{11}f_1 + L_{12}f_2)f_1$, also expressed in terms of Onsager coefficients L_{1i} 's given by

$$L_{11} = \frac{m}{T_1\tau(e^{\gamma\tau} - 1)} \left[(e^{\gamma\tau} - 1) \int_0^{\tau/2} h_1(t)e^{-\gamma t} \int_0^t h_1(t')e^{\gamma t'} dt' dt + \int_0^{\tau/2} h_1(t)e^{-\gamma t} dt \int_0^{\tau/2} h_1(t')e^{\gamma t'} dt' \right],$$

$$L_{12} = \frac{m}{T_1\tau(e^{\gamma\tau} - 1)} \int_0^{\tau/2} h_1(t)e^{-\gamma t} dt \int_{\tau/2}^{\tau} h_2(t')e^{\gamma t'} dt'. \quad (22)$$

Reciprocal relations for cross coefficients L_{12} and L_{21} are derived when drivings are reversed and indices $1 \leftrightarrow 2$ exchanged [21,38]. The linear contribution \mathcal{P}_α can also be expressed in the following generic form:

$$\mathcal{P}_\alpha = T_2 f_2 (\tilde{L}_{222} f_2^2 + \tilde{L}_{211} f_1^2 + \tilde{L}_{221} f_2 f_1), \quad (23)$$

where general expressions for coefficients \tilde{L}_{2jk} 's are listed in Appendix A 1 (A 2) for generic (constant and linear drivings), respectively. However, in contrast to Onsager ones, the above coefficients \tilde{L}_{ijk} 's do not necessarily satisfy the standard reciprocal relations [20,21,38]. Analogous to \mathcal{P}_α , the linear contribution for $\overline{W}_{1\alpha}$ can also be expressed in following form given by $\overline{W}_{1\alpha} = T_1 f_1 (\tilde{L}_{111} f_1^2 + \tilde{L}_{221} f_2^2 + \tilde{L}_{112} f_2 f_1)$, whose coefficients \tilde{L}_{1jk} 's are also listed in Appendix A 1. From Eq. (23), the optimal force f_{2P} providing maximum power \mathcal{P}_P is straightforwardly obtained and given by

$$f_{2P} = \frac{-(L_{22} + \alpha f_1 \tilde{L}_{221})}{3\alpha \tilde{L}_{222}} \left[1 - \sqrt{1 - \frac{3\alpha f_1 \tilde{L}_{222} (L_{21} + \alpha f_1 \tilde{L}_{221})}{(L_{22} + \alpha f_1 \tilde{L}_{221})^2}} \right], \quad (24)$$

with associate \mathcal{P}_P reading

$$\frac{\mathcal{P}_P}{T_2} = \frac{2(\alpha f_1 \tilde{L}_{221} + L_{22})^2 (\alpha f_1 \tilde{L}_{221} + L_{22} - \mathcal{A}) - 3\alpha f_1 \tilde{L}_{222} (\alpha f_1 \tilde{L}_{211} + L_{21}) (3\alpha f_1 \tilde{L}_{221} + 3L_{22} - 2\mathcal{A})}{27\alpha^2 \tilde{L}_{222}^2},$$

respectively, where parameter \mathcal{A} reads $\mathcal{A} = \sqrt{(\alpha f_1 \tilde{L}_{221} + L_{22})^2 - 3\alpha f_1 \tilde{L}_{222} (\alpha f_1 \tilde{L}_{211} + L_{21})}$. Note that one recovers expressions $2f_{2P} = -L_{21}/L_{22}$ and $\mathcal{P}_P = T_2 L_{21}^2 f_1 / 4L_{22}$ as $\alpha = 0$.

D. Approximate descriptions for maximum efficiencies

Since the average heat components \overline{Q}_{1f} and \overline{Q}_{2f} are always positive, the system solely will receive heat from the i th thermal bath from a temperature difference ΔT in which $\overline{Q}_i = \overline{Q}_{if} + \overline{Q}_{f_1, f_2, T_i} < 0$. Giving that the above condition is always fulfilled for large ΔT and by the fact that the power output \mathcal{P} does not depend on the temperatures, the efficiency of thermal engines for $\alpha = 0$ always decreases when compared to its corresponding work-to-work converter $\eta_{wtw} = -\mathcal{P}/\overline{W}_1$. However, a coupling between drivings and velocities makes it possible to (properly) adjust the coupling ensuring a maximum efficiency. Despite the complex interplay between α and f_1, f_2 leading to very cumbersome expressions for maximized quantities (above all the efficiency), it is possible to predict optimized expressions for efficiency by means of two simple reasonings, described as follows: the first is similar to the previous one in which one assumes the following expansions for \overline{Q}_1 and \overline{Q}_2 :

$$\overline{Q}_1 = \overline{Q}_{10} + \alpha \tilde{Q}_{1\alpha}, \quad \overline{Q}_2 = \overline{Q}_{20} + \alpha \tilde{Q}_{2\alpha}. \quad (25)$$

By inserting the above expressions in Eq. (19) and considering up to the linear term, the efficiency is also given by $\eta \approx \eta_0 + \alpha \eta_\alpha$, where η_0 and η_α read

$$\eta_0 = -\frac{\mathcal{P}_0}{\overline{W}_{10} + \overline{Q}_{10}\Theta(-\overline{Q}_{10}) + \overline{Q}_{20}\Theta(-\overline{Q}_{20})} \quad (26)$$

and

$$\eta_\alpha = \frac{\mathcal{P}_\alpha - \eta_0 [\overline{W}_{1\alpha} + \overline{Q}_{1\alpha}\Theta(-\overline{Q}_{10}) + \overline{Q}_{2\alpha}\Theta(-\overline{Q}_{20})]}{\overline{W}_{10} + \overline{Q}_{10}\Theta(-\overline{Q}_{10}) + \overline{Q}_{20}\Theta(-\overline{Q}_{20})}, \quad (27)$$

respectively. Note that η_0 solely depends on zeroth order quantities (as expected), whereas η_α depends on η_0 , $\overline{W}_{i\alpha}$'s, and $\overline{Q}_{i\alpha}$'s. Maximization of η with respect to f_2 , providing f_{2mE} , can be calculated from Eqs. (26) and (27).

Although providing a first insight about the influence of α , Eqs. (24)–(27) are very cumbersome and rather few are instructive. Contrariwise, for the case in which the above approximation (for small α) is not valid, maximization of efficiency can be carried out by means of a simple argument, as described as follows: let us consider the situation in which the power output monotonically increases (this is promptly verified for the drivings considered here) upon α being varied. In such a case, the efficiency can be enhanced by searching for the optimal coupling α_E , in which the net exchanged heat \overline{Q}_i , given by $\overline{Q}_{if} + \overline{Q}_{f_1, f_2, T_i}$, vanishes. In certain cases, the average heat component $\overline{Q}_{f_1, f_2, T_i}$ dominates over \overline{Q}_{if} ($|\overline{Q}_{f_1, f_2, T_i}| \gg \overline{Q}_{if}$). Although this is verified for sufficiently large $|\Delta T|$ and fixed f_1, f_2 , such a condition can be fulfilled for other interplay among parameters. Hence, from Eq. (17), when this is indeed the case, the optimal coupling α_E is given by

$$\alpha_E = \frac{T_1 - T_2}{f_1 T_2 - f_2 T_1}. \quad (28)$$

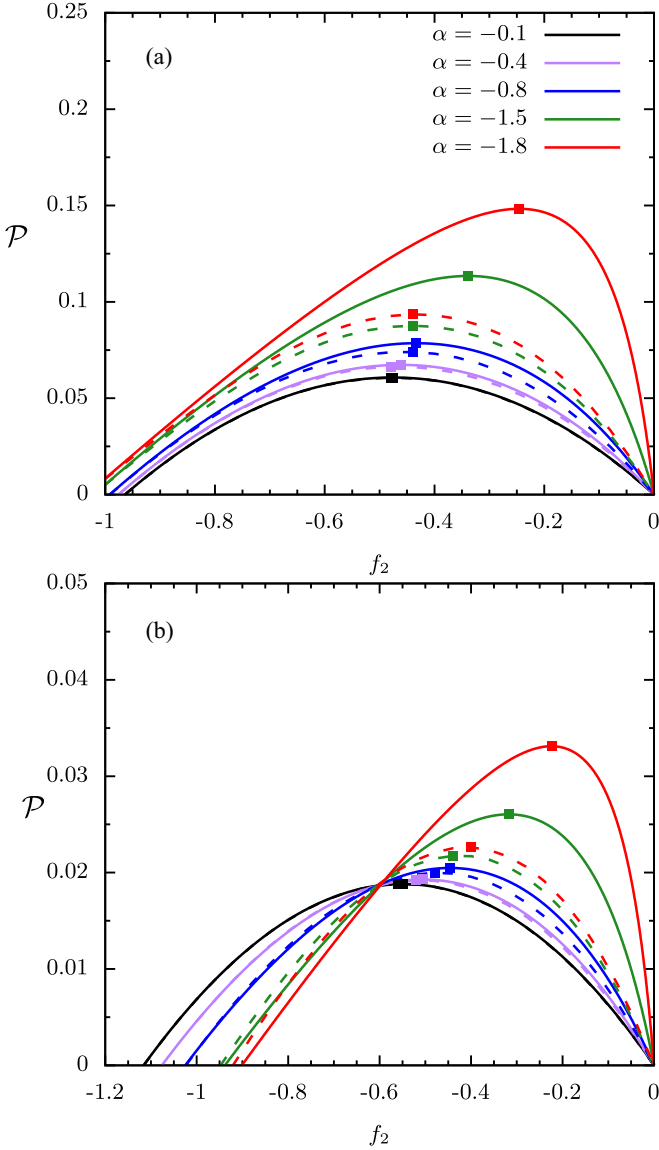


FIG. 1. For constant (a) and linear (b) drivings, the depiction of power output \mathcal{P} (continuous) and those from a linear analysis (dashed), where squares correspond to f_{2p} 's ensuring maximum power \mathcal{P}_p 's. Parameters: $m = \tau = \gamma = 1$; $f_1 = 1$.

Note that such an above approximate expression for α_E is general and expresses the interplay among driving strengths and temperatures and approaches zero as $\Delta T \rightarrow 0$ for finite $f_1 - f_2$. Thus it suggests that forces proportional to the velocity can increase the efficiency under a suited choice of temperatures and forces, in which the corresponding maximum efficiency $\eta_{\alpha_E, f_1, f_2, \Delta T}$ reduces to the work-to-work converter expression:

$$\bar{\eta}_{f_2, f_1, \Delta T} = -\frac{\mathcal{P}_E^*}{\bar{W}_{1E}^*}, \quad (29)$$

with $\mathcal{P}_E^* = \mathcal{P}(f_1, f_2, \Delta T, \tau)$ and $\bar{W}_{1E}^* = \bar{W}_1(f_1, f_2, \Delta T, \tau)$ denoting the \mathcal{P} and \bar{W}_1 evaluated at $\alpha = \alpha_E$. Note that Eq. (29) solely depends on f_1 , f_2 , τ , and ΔT . The efficiency can also be maximized with respect to f_2 (for fixed ΔT) or ΔT (for fixed f_2). Although it can be directly carried out by a

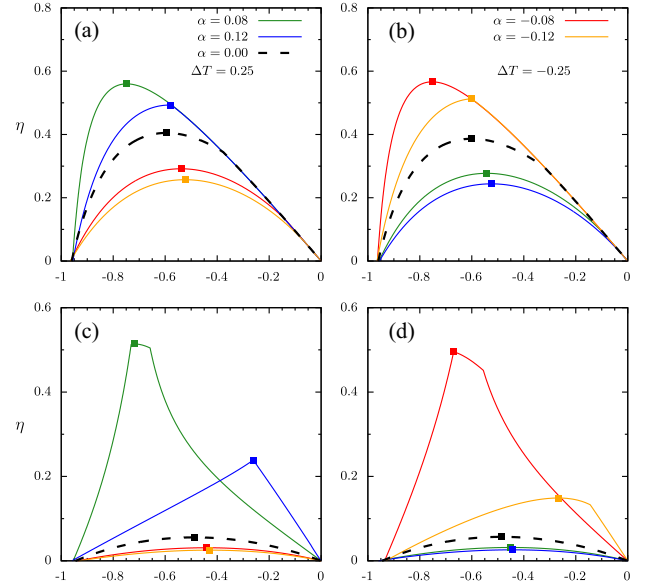


FIG. 2. For constant (top) and linear (bottom) drivings, the depiction of efficiency η for representative values of α and distinct ΔT 's. In (a)/(c) and (b)/(d), T_1 reads $T_1 = 2.0$ and $T_1 = 1.75$, respectively. Squares denote the associate maximum efficiencies (with respect to the f_2). Parameters: $m = \tau = \gamma = f_2 = 1$.

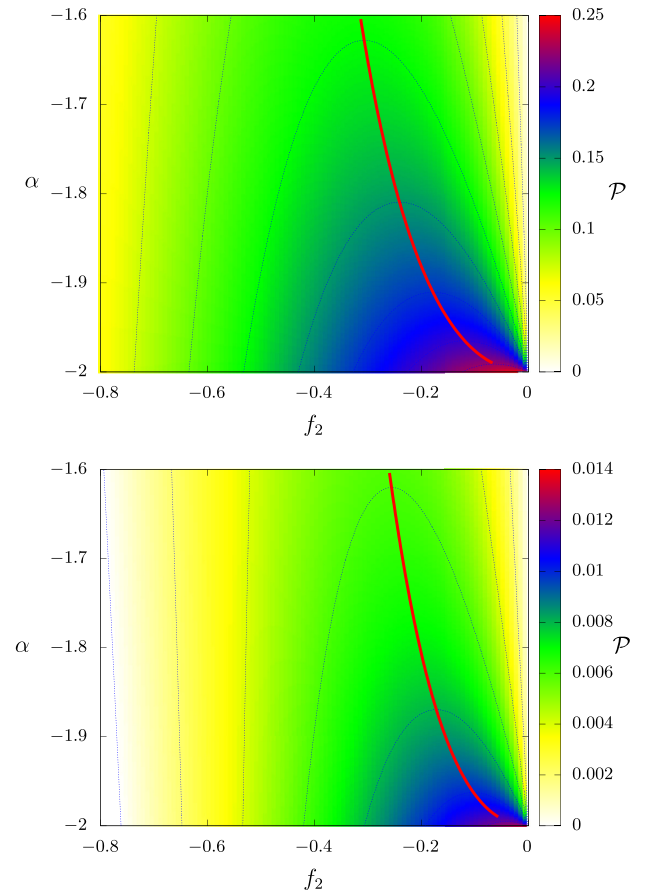


FIG. 3. For constant (top) and linear (bottom) drivings, the depiction of power output \mathcal{P} in the plane (f_2, α) . For each α , red lines denote the locus (f_{2p}, \mathcal{P}_p) of maximum \mathcal{P} with respect to f_2 . Parameters: $m = \tau = \gamma = 1$; $f_1 = 1$.

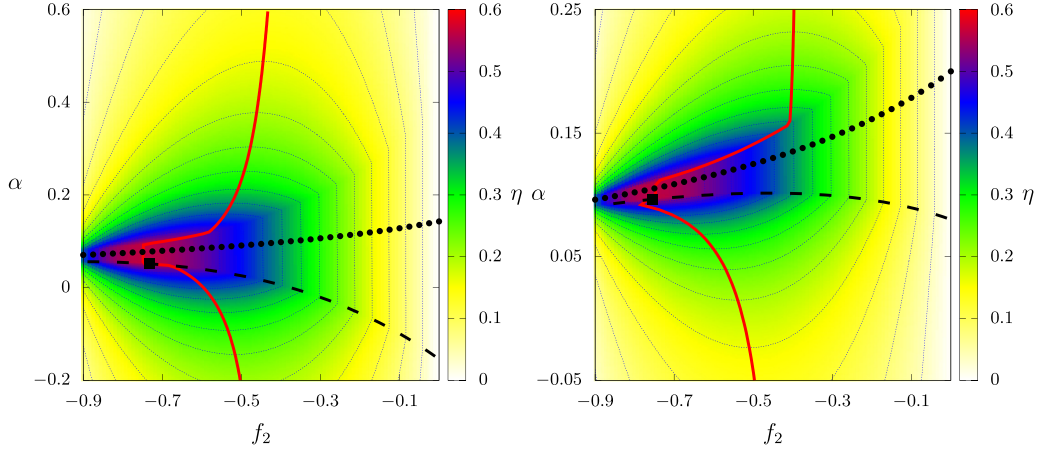


FIG. 4. For the same parameters of Fig. 2, the efficiency phase diagrams α versus f_2 for $\Delta T = 0.25$ (left) and -0.25 (right) for constant drivings. Continuous, dashed, and dotted lines correspond to the maximization with respect to f_2 (fixed α), α (fixed f_2), and approximate [from Eq. (28)], respectively. “Squares” denote the simultaneous maximization with respect to α and f_2 .

simultaneous maximization of Eq. (19), an approximate expression for (simultaneous) maximum efficiency $\eta_{f_1, \theta}^*$ ($\theta = f_2$ or ΔT) is obtained by searching for f_2 or ΔT that maximizes Eq. (29):

$$\eta_{f_1, \theta}^* = -\frac{\mathcal{P}_{mE}^*}{\bar{W}_{1mE}^*}, \quad (30)$$

where $\mathcal{P}_{mE}^* = \mathcal{P}(f_1, \theta_E, \tau)$ and $\bar{W}_{1mE}^* = \bar{W}_1(f_1, \theta_E, \tau)$ denote the \mathcal{P} and \bar{W}_1 evaluated at $\alpha = \alpha_E$ and $f_2 = f_{2E}(\theta = \Delta T)$ or $\Delta T = \Delta T_E$ ($\theta = f_2$), respectively.

III. RESULTS

In all cases, analysis will be carried out for constant and linear drivings and the following parameter choices $m = \tau = \gamma = f_1 = 1$. Expressions for Onsager and coefficients from the linear analysis are listed in Appendix A 2. In the first round of analysis, the influence of α over the power output \mathcal{P} and efficiency η is exemplified for some sets of parameters,

as depicted in Figs. 1 and 2 for constant and linear drivings. \mathcal{P} (Fig. 1) monotonically increases with the absolute value of α , having this feature captured by the linear analysis for small α . Consequently, apart from the increase of power as the absolute value of α increases, there is no optimal coupling leading to maximum power, implying its maximization solely with respect to the force f_2 in which \mathcal{P}_P .

The influence of α over the efficiency is more revealing and exemplified in Fig. 2 for two representative temperature differences: $\Delta T = 0.25$ ($T_1 > T_2$) and $\Delta T = -0.25$ ($T_1 < T_2$). In both cases, efficiencies are rather small when $\alpha = 0$ (couplingless case) and an optimal coupling between driving and velocities ensures their substantial increases (see, e.g., dashed lines). Also, efficiency curves behave quite differently with respect to $\alpha = 0$. This is due to the influence of parameters (mainly f_2 , α , and ΔT) on \mathcal{P}/\bar{W}_1 and the amount of a received heat [see, e.g., the denominator from Eq. (19)] and it is more significant for linear drivings (see, e.g., Fig. 2), where efficiencies are just smaller [20,22]. While \mathcal{P} and \bar{W}_1^* always increase with the absolute value of α , there is an optimal

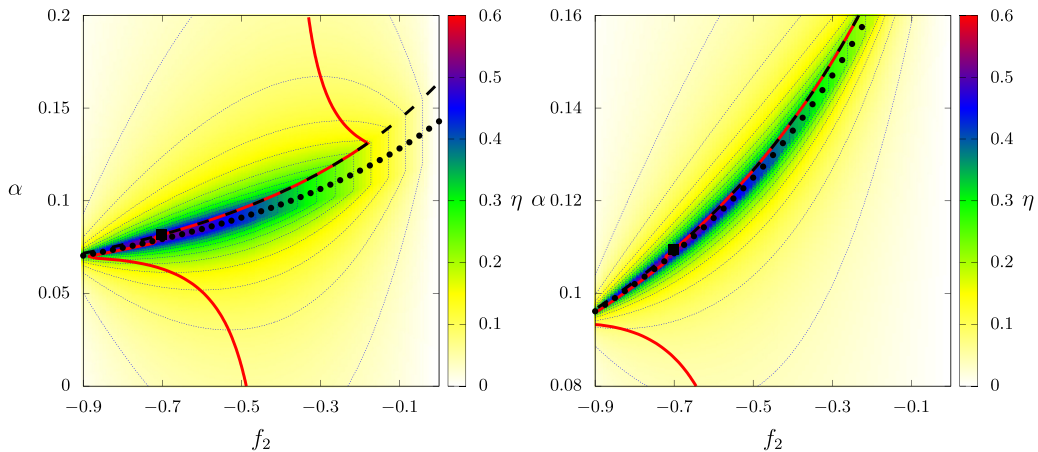


FIG. 5. For the same parameters of Fig. 2, the efficiency phase diagrams α versus f_2 for $\Delta T = 0.25$ (left) and -0.25 (right) for linear drivings. Continuous, dashed, and dotted lines correspond to the maximization with respect to f_2 (fixed α), α (fixed f_2), and approximate [from Eq. (28)], respectively. “Squares” denote the simultaneous maximization with respect to α and f_2 .

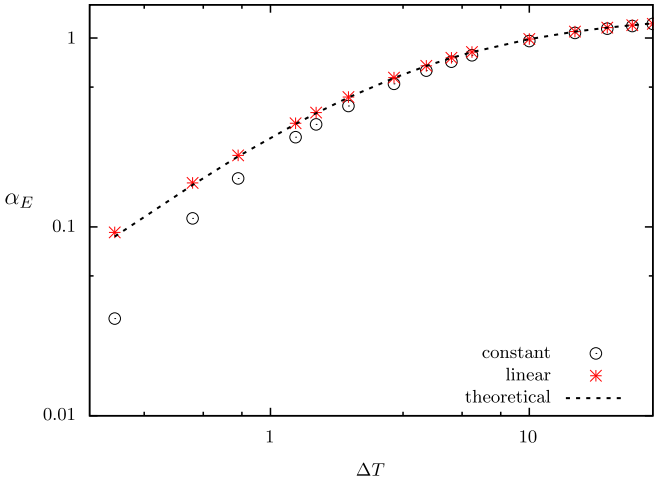


FIG. 6. Comparison among logarithm plots of α_E obtained from Eq. (28) (dashed lines) and from direct maximization of Eq. (19) for constant (circles) and linear (stars) drivings. Parameters: $T_2 = 1.5$, $m = \tau = \gamma = 1$, $f_1 = 1$, and $f_2 = -0.75$.

coupling α_E controlling and decreasing the amount of “wasted” average heat and thereby providing a larger efficiency. In particular, the optimal coupling α_E is positive and negative for $T_1 > T_2$ and $T_1 < T_2$, respectively.

For the above set of parameters, a global overview about the role of α is shown in Figs. 3–5 for heat maps (phase diagrams) of \mathcal{P} and η for linear and constant drivings. As in Fig. 1, \mathcal{P} monotonically increases with the coupling and providing, for all values of α , optimal f_{2P} 's ensuring maximal \mathcal{P}_P (red lines). Contrasting to the power output, in which a simultaneous maximization of power is not possible, efficiencies' phase diagrams (Figs. 4 and 5) exhibit a central region in which it is simultaneously maximized. Maximum lines behave differently, reflecting the distinct dependence between η with α and f_2 . They meet at the vicinity of global maximum. Approximate curves (dotted lines), obtained from Eq. (28), approach to exact ones (dashed) as $|\Delta T|$ is raised. They are always closer to each other for linear than for constant drivings. The reliability of Eq. (28) is reinforced and complemented in Fig. 6, in which the optimal α_E approaches that obtained from the direct maximization of efficiency as $|\Delta T|$ rises. Figure 7 compares maximum efficiencies obtained from direct maximization of Eq. (19) with $\bar{\eta}_{f_2, f_1, \Delta T}$ and $\eta_{f_1, \Delta T}^*$, given by Eqs. (29) and (30), respectively. Note the excellent agreement between exact and approximate expressions (deviations among curves are almost imperceptible), reinforcing the search for optimal parameters for maximum efficiencies. At the vicinity of optimal couplings, they are substantially larger than $\bar{\eta}_{f_1, \Delta T} = 0.4049/0.0555$ and $0.1822/0.0151$ (see, e.g., Fig. 2), obtained for the couplingless constant and linear cases for $\Delta T = 0.25$ and 1, respectively.

Finally, the influence of temperature sets is illustrated in Fig. 8 for constant drivings [similar results (not shown) are obtained for linear drivings] for $T_1 = T_2 + \Delta T$ and $T_2 = 1$. At least for the set of parameters considered, a simultaneous maximization of efficiency (with respect to ΔT and f_2) is absent and only the maximization with respect to f_2 can be carried. However, the coupling allows a suitable choice of

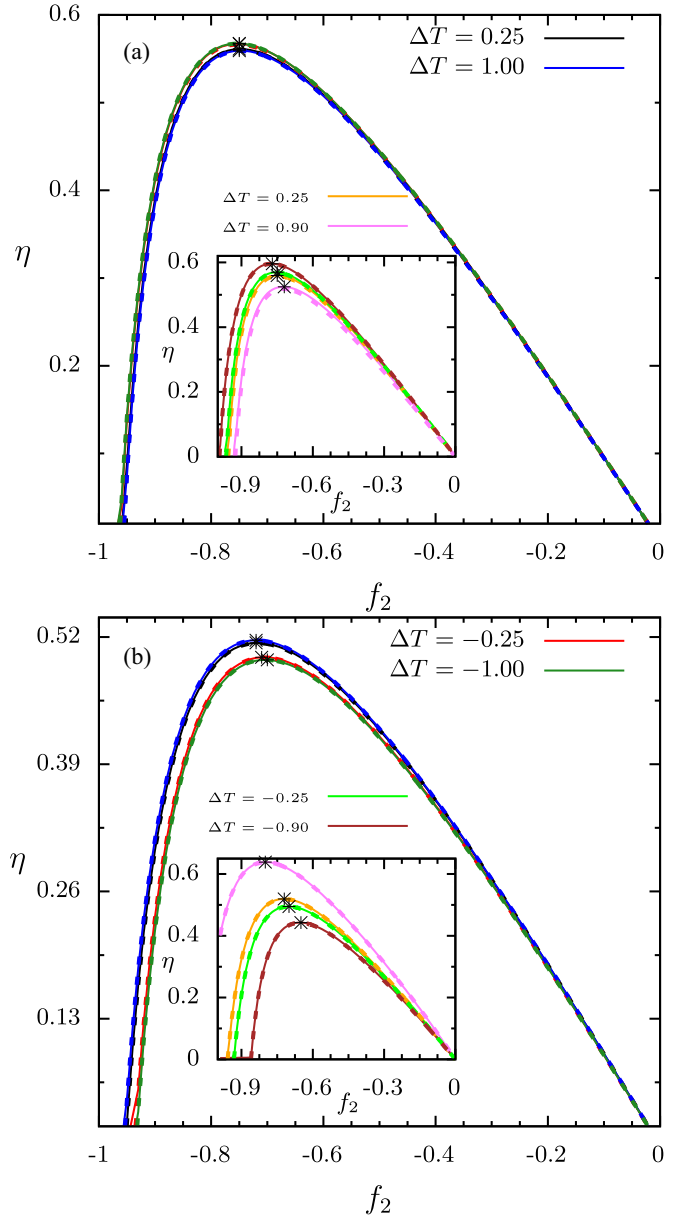


FIG. 7. For the same parameters from Figs. 4 and 5, the main panels show efficiency maxima $\bar{\eta}_{f_2, f_1, \Delta T}$ versus f_2 for distinct ΔT 's for constant (top) and linear (bottom) drivings, respectively. Inset: results for the same ΔT but for $T_1 = 0.1, 1, 1$, and 1.25 , respectively. Stars denote the prediction from Eq. (30) for maximized efficiencies $\bar{\eta}_{\theta, f_1}^*$'s. Continuous and dashed lines correspond to exact and efficiencies evaluated from Eq. (29), respectively.

temperature difference in order to enhance the system performance or even project it with a desirable power and efficiency.

IV. CONCLUSIONS

Collisional Brownian engines constitute a very simple class of machines having thermodynamic properties exactly obtained, irrespective the driving, temperature of thermal baths, and the duration of each stage. Notwithstanding, its performance can decrease substantially depending on the way it is projected (period, duration of stage, temperature of baths,

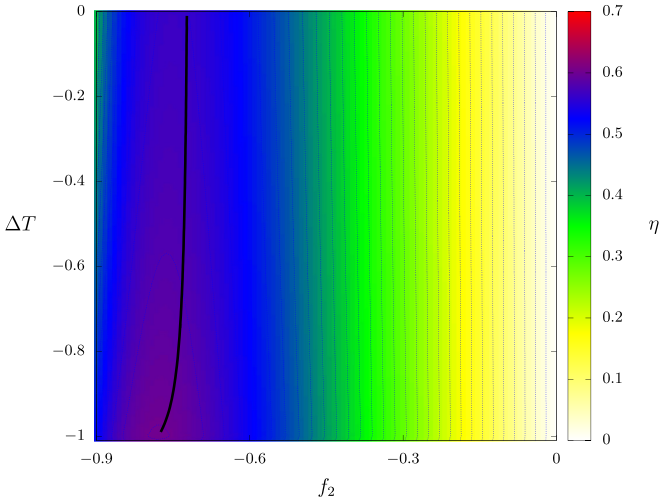


FIG. 8. For constant drivings, the efficiency phase diagram ΔT versus f_2 . Continuous line denotes the maximization with respect to the f_2 (fixed ΔT). Parameters: $T_1 = T_2 + \Delta T$ and $T_2 = 1$.

and drivings). In order to address possible improvements in such class of systems, we introduced a velocity driving component and its influence was analyzed from the framework of stochastic thermodynamics. Results for constant and linear drivings reveal that it can be conveniently considered in order to optimize efficiency, even for large temperature differences

between thermal reservoirs, where the couplingless engine operates very inefficiently. Distinct maximization routes were considered and substantial improvements can be gained. Despite the absence of a simultaneous maximization for the power output for constant and linear drivings, we underscore a reliable choice of coupling α for ensuring a compromise between the power output and efficiency.

As potential perspectives of the present work, it might be interesting to address other kinds of maximizations, such as by holding the dissipation fixed as well as the influence of the coupling between driving and velocity in such cases. The extension of our collisional approach for massive Brownian particles also constitutes an interesting extension, in order to compare the performances of such engines. Finally, recent results [37,39] have addressed new mechanisms for the selection of certain states, by considering time variations of the temperature. A simpler alternative might be changing the temperature under a sequential approach, such as those considered in the present manuscript.

ACKNOWLEDGMENTS

We acknowledge Pedro E. Harunari for useful comments and for pointing us out Ref. [25]. I.N.M. and C.E.F. acknowledge the financial support from FAPESP under Grants No. 2021/12551-8 and No. 2021/03372-2, respectively. The financial support from CNPq and CAPES is also acknowledged.

APPENDIX

1. Coefficients of the linear approximation for small couplings

Below, we list the expressions for coefficients \tilde{L}_{ijk} 's from the linear expansion of \mathcal{P} and \bar{W}_1 for generic drivings $h_1(t)$ and $h_2(t)$:

$$\tilde{L}_{111} = \frac{\alpha}{2\tau T_1} \int_0^{\frac{\tau}{2}} e^{-\gamma t} \left[\frac{\mathcal{F}_1\left(\frac{\tau}{2}, 0\right) [e^{\gamma\tau}(2t + \tau) - 2t]}{(e^{\gamma\tau} - 1)^2} + 2t\mathcal{F}_1(t, 0) \right] dt, \quad (\text{A1})$$

$$\tilde{L}_{112} = \frac{\alpha e^{\frac{3\gamma\tau}{4}} \sinh\left(\frac{\gamma\tau}{4}\right)}{\gamma^2\tau(e^{\gamma\tau} - 1)^2 T_1} \left\{ \gamma\tau\mathcal{F}_1\left(\frac{\tau}{2}, 0\right) + \mathcal{F}_2(\tau, 0) \left[4 \sinh\left(\frac{\gamma\tau}{2}\right) - \gamma\tau \right] \right\}, \quad (\text{A2})$$

$$\tilde{L}_{122} = \frac{\alpha e^{\gamma\tau} (e^{\frac{\gamma\tau}{2}} - 1) \mathcal{F}_2(\tau, 0)}{2\gamma(e^{\gamma\tau} - 1)^2 T_1}, \quad (\text{A3})$$

$$\tilde{L}_{222} = \frac{\alpha}{2\tau(e^{\gamma\tau} - 1)^2 T_2} \int_{\frac{\tau}{2}}^{\tau} e^{\frac{1}{2}\gamma(\tau-2t)} [\mathcal{F}_2(\tau, 0) [2t(e^{\gamma\tau} - 1) + \tau] - (e^{\gamma\tau} - 1)^2 (\tau - 2t) \mathcal{F}_2(t, 0)] dt, \quad (\text{A4})$$

$$\tilde{L}_{221} = \frac{\alpha [\coth\left(\frac{\gamma\tau}{4}\right) - 1] \text{sech}^2\left(\frac{\gamma\tau}{4}\right) \left\{ \mathcal{F}_1\left(\frac{\tau}{2}, 0\right) [4 \sinh\left(\frac{\gamma\tau}{2}\right) - \gamma\tau] + \gamma\tau \mathcal{F}_2(\tau, 0) \right\}}{16\gamma^2\tau T_2}, \quad (\text{A5})$$

and

$$\tilde{L}_{211} = \frac{\alpha e^{\gamma\tau} (e^{\frac{\gamma\tau}{2}} - 1) \mathcal{F}_1\left(\frac{\tau}{2}, 0\right)}{2\gamma(e^{\gamma\tau} - 1)^2 T_2}. \quad (\text{A6})$$

2. Coefficients of the linear approximation for constant and linear drivings

As stated in the main text, by inserting explicit expressions for drivings $h_1(t)$ and $h_2(t)$, Onsager coefficients L_{ij} 's and coefficients \tilde{L}_{ijk} 's can be straightforwardly obtained from Eqs. (21) and (22) and (A1)–(A6), respectively. For constant drivings,

we arrive at the following expressions:

$$T_1 L_{11} = T_2 L_{22} = \frac{1}{\gamma} \left(\frac{1}{2} - \frac{\tanh\left(\frac{\gamma\tau}{4}\right)}{\gamma\tau} \right), \quad T_1 L_{12} = T_2 L_{21} = \frac{1}{\gamma^2 \tau} \tanh\left(\frac{\gamma\tau}{4}\right) \quad (\text{A7})$$

for Onsager ones and

$$T_1 \tilde{L}_{111} = T_2 \tilde{L}_{222} = \frac{\gamma\tau [\text{sech}^2\left(\frac{\gamma\tau}{4}\right) + 4] - 16 \tanh\left(\frac{\gamma\tau}{4}\right)}{8\gamma^3 \tau}, \quad (\text{A8})$$

$$T_1 \tilde{L}_{122} = T_2 \tilde{L}_{211} = \frac{[4 \sinh\left(\frac{\gamma\tau}{2}\right) - \gamma\tau] \text{sech}^2\left(\frac{\gamma\tau}{4}\right)}{8\gamma^3 \tau}, \quad (\text{A9})$$

$$T_1 \tilde{L}_{112} = T_2 \tilde{L}_{221} = \frac{\tanh\left(\frac{\gamma\tau}{4}\right)}{\gamma^3 \tau} \quad (\text{A10})$$

for the linear contribution of α . Similarly, for linear drivings, their expressions are listed below:

$$T_1 L_{11} = T_2 L_{22} = \frac{\gamma\tau(\gamma\tau - 2) + 2(4 - \gamma\tau) \tanh\left(\frac{\gamma\tau}{4}\right)}{8\gamma^3 \tau}, \quad T_1 L_{12} = T_2 L_{21} = \frac{(\gamma\tau - 4) \tanh\left(\frac{\gamma\tau}{4}\right) + \gamma\tau}{4\gamma^3 \tau} \quad (\text{A11})$$

for Onsager ones and

$$T_1 \tilde{L}_{111} = \frac{-\gamma^2 \tau^2 + e^{\frac{3\gamma\tau}{2}} [\gamma\tau(\gamma\tau - 8) + 24] + e^{\gamma\tau} [\gamma\tau(\gamma\tau - 4) - 24] - 3e^{\frac{\gamma\tau}{2}} [\gamma\tau(\gamma\tau - 4) + 8] + 24}{8\gamma^4 \tau (e^{\frac{\gamma\tau}{2}} - 1)(e^{\frac{\gamma\tau}{2}} + 1)^2}, \quad (\text{A12})$$

$$T_1 \tilde{L}_{122} = T_2 \tilde{L}_{211} = \frac{(e^{\frac{\gamma\tau}{2}} - 1) [2e^{\frac{3\gamma\tau}{2}} (\gamma\tau - 4) + 2e^{\gamma\tau} (\gamma\tau + 4) + e^{\frac{\gamma\tau}{2}} [\gamma\tau(\gamma\tau - 4) + 8] - 8]}{4\gamma^4 \tau (e^{\gamma\tau} - 1)^2}, \quad (\text{A13})$$

and

$$T_1 \tilde{L}_{112} = T_2 \tilde{L}_{221} = \frac{[\gamma\tau + (\gamma\tau - 4) \tanh\left(\frac{\gamma\tau}{4}\right)]}{4\gamma^4 \tau} \quad (\text{A14})$$

for the linear contribution in α .

-
- [1] H. B. Callen, *Thermodynamics and an Introduction to Thermostatistics* (John Wiley & Sons, New York, 1985).
- [2] C. Van den Broeck, *Phys. Rev. Lett.* **95**, 190602 (2005).
- [3] U. Seifert, *Rep. Prog. Phys.* **75**, 126001 (2012).
- [4] S. Rana, P. S. Pal, A. Saha, and A. M. Jayannavar, *Phys. Rev. E* **90**, 042146 (2014).
- [5] I. A. Martínez, É. Roldán, L. Dinis, D. Petrov, J. M. Parrondo, and R. A. Rica, *Nat. Phys.* **12**, 67 (2016).
- [6] S. Liepelt and R. Lipowsky, *Phys. Rev. Lett.* **98**, 258102 (2007).
- [7] S. Liepelt and R. Lipowsky, *Phys. Rev. E* **79**, 011917 (2009).
- [8] J. D. Seader, *Thermodynamic Efficiency of Chemical Processes* (The MIT Press, Cambridge, MA, 1982).
- [9] M. Esposito, R. Kawai, K. Lindenberg, and C. Van den Broeck, *Phys. Rev. E* **81**, 041106 (2010).
- [10] J. A. Albay, Z.-Y. Zhou, C.-H. Chang, and Y. Jun, *Sci. Rep.* **11**, 4394 (2021).
- [11] K. Proesmans, Y. Dreher, M. Gavrilov, J. Bechhoefer, and C. Van den Broeck, *Phys. Rev. X* **6**, 041010 (2016).
- [12] N. Golubeva and A. Imparato, *Phys. Rev. Lett.* **109**, 190602 (2012).
- [13] I. N. Mamede, P. E. Harunari, B. A. N. Akasaki, K. Proesmans, and C. E. Fiore, *Phys. Rev. E* **105**, 024106 (2022).
- [14] Y. Jun, M. Gavrilov, and J. Bechhoefer, *Phys. Rev. Lett.* **113**, 190601 (2014).
- [15] C. H. Bennett, *Int. J. Theor. Phys.* **21**, 905 (1982).
- [16] K. Maruyama, F. Nori, and V. Vedral, *Rev. Mod. Phys.* **81**, 1 (2009).
- [17] T. Sagawa, *J. Stat. Mech.* (2014) P03025.
- [18] J. M. Parrondo, J. M. Horowitz, and T. Sagawa, *Nat. Phys.* **11**, 131 (2015).
- [19] P. E. Harunari, F. S. Filho, C. E. Fiore, and A. Rosas, *Phys. Rev. Res.* **3**, 023194 (2021).
- [20] C. E. F. Noa, A. L. L. Stable, W. G. C. Oropesa, A. Rosas, and C. E. Fiore, *Phys. Rev. Res.* **3**, 043152 (2021).
- [21] F. S. Filho, B. A. N. Akasaki, C. E. F. Noa, B. Cleuren, and C. E. Fiore, *Phys. Rev. E* **106**, 044134 (2022).
- [22] A. L. L. Stable, C. E. F. Noa, W. G. C. Oropesa, and C. E. Fiore, *Phys. Rev. Res.* **2**, 043016 (2020).
- [23] C. Ganguly and D. Chaudhuri, *Phys. Rev. E* **88**, 032102 (2013).
- [24] F. Schweitzer, W. Ebeling, and B. Tilch, *Phys. Rev. Lett.* **80**, 5044 (1998).
- [25] S. Dago, J. Pereda, S. Ciliberto, and L. Bellon, *J. Stat. Mech.* (2022) 053209.
- [26] J. R. Howse, R. A. L. Jones, A. J. Ryan, T. Gough, R. Vafabakhsh, and R. Golestanian, *Phys. Rev. Lett.* **99**, 048102 (2007).
- [27] W. F. Paxton, K. C. Kistler, C. C. Olmeda, A. Sen, S. K. St. Angelo, Y. Cao, T. E. Mallouk, P. E. Lammert, and V. H. Crespi, *J. Am. Chem. Soc.* **126**, 13424 (2004).

- [28] F. Schweitzer and J. D. Farmer, *Brownian Agents and Active Particles: Collective Dynamics in the Natural and Social Sciences* (Springer, New York, 2003), Vol. 1.
- [29] T. Tomé and M. J. De Oliveira, *Stochastic Dynamics and Irreversibility* (Springer, Cham, 2015).
- [30] T. Tomé and M. J. de Oliveira, *Phys. Rev. E* **82**, 021120 (2010).
- [31] T. Tomé and M. J. de Oliveira, *Phys. Rev. E* **91**, 042140 (2015).
- [32] M. Esposito and C. Van den Broeck, *Phys. Rev. E* **82**, 011143 (2010).
- [33] K. Proesmans, C. Driesen, B. Cleuren, and C. Van den Broeck, *Phys. Rev. E* **92**, 032105 (2015).
- [34] H. Vroylandt, M. Esposito, and G. Verley, *Europhys. Lett.* **120**, 30009 (2017).
- [35] T. Herpich, J. Thingna, and M. Esposito, *Phys. Rev. X* **8**, 031056 (2018).
- [36] T. Herpich and M. Esposito, *Phys. Rev. E* **99**, 022135 (2019).
- [37] D. M. Busiello and C. E. Fiore, *J. Phys. A* **55**, 485004 (2022).
- [38] A. Rosas, C. Van den Broeck, and K. Lindenberg, *Phys. Rev. E* **97**, 062103 (2018).
- [39] D. M. Busiello, S. Liang, F. Piazza, and P. De Los Rios, *Commun. Chem.* **4**, 16 (2021).